Eur Radiol (2008) 18: 1251–1259
DOI 10.1007/s00330-008-0859-3

Siegfried Trattnig
Tallal C. Mamisch
Katja Pinker
Stephan Domayer
Pavol Szomolanyi
Stefan Marlovits
Florian Kutscha-Lissberg
Goetz H. Welsch

Differentiating normal hyaline cartilage from post-surgical repair tissue using fast gradient echo imaging in delayed gadolinium-enhanced MRI (dGEMRIC) at 3 Tesla

Received: 24 October 2007
Revised: 12 December 2007
Accepted: 31 December 2007
Published online: 2 February 2008

S. Trattnig (✉) · K. Pinker · S. Domayer · P. Szomolanyi · G. H. Welsch
MR Center-High field MR, Department of Radiology, Medical University of Vienna, Lazarettgasse 14, A-1090 Vienna, Austria
e-mail: siegfried.trattnig@meduniwien.ac.at
Tel.: +43-1-404001773
Fax: +43-1-404007631

T. C. Mamisch
Orthopedic Surgery Department, Inselspital Bern, Bern, Switzerland

S. Domayer
Department of Orthopaedics, Medical University of Vienna, Vienna, Austria

P. Szomolanyi
Department of Imaging Methods, Institute of Measurement Science, Slovak Academy of Sciences, Bratislava, Slovak Republic

S. Marlovits · F. Kutscha-Lissberg
Department of Traumatology, Center for Joints and Cartilage, Medical University of Vienna, Vienna, Austria

Abstract The purpose was to evaluate the relative glycosaminoglycan (GAG) content of repair tissue in patients after microfracturing (MFX) and matrix-associated autologous chondrocyte transplantation (MACT) of the knee joint with a dGEMRIC technique based on a newly developed short 3D-GRE sequence with two flip angle excitation pulses. Twenty patients treated with MFX or MACT (ten in each group) were enrolled. For comparability, patients from each group were matched by age (MFX: 37.1±16.3 years; MACT: 37.4±8.2 years) and postoperative interval (MFX: 33.0±17.3 months; MACT: 32.0±17.2 months). The Δ relaxation rate (ΔR1) for repair tissue and normal hyaline cartilage and the relative ΔR1 were calculated, and mean values were compared between both groups using an analysis of variance. The mean ΔR1 for MFX was 1.07±0.34 versus 0.32±0.20 at the intact control site, and for MACT, 1.90±0.49 compared to 0.87±0.44, which resulted in a relative ΔR1 of 3.39 for MFX and 2.18 for MACT. The difference between the cartilage repair groups was statistically significant. The new dGEMRIC technique based on dual flip angle excitation pulses showed higher GAG content in patients after MACT compared to MFX at the same postoperative interval and allowed reducing the data acquisition time to 4 min.

Keywords dGEMRIC · Articular cartilage · Matrix-associated autologous chondrocyte transplantation · Microfracture · MRI at 3 T

Introduction

Glycosaminoglycans (GAG) are negatively charged side chains of proteoglycan in articular cartilage and are therefore the main source of fixed charge density (FCD) in cartilage, and are often lost in the early stage of cartilage degeneration [1, 2]. Intravenously administered gadolinium diethylenetriamine pentaacetate anion (Gd-DTPA^{2-}) shows an influx from the joint space into cartilage until equilibrium between both compartments is achieved. This equilibrium is in inverse relation to the FCD, which is, in turn, directly related to the GAG concentration; therefore, T1, which is determined by the Gd-DTPA^{2-} concentration, becomes a specific measure of tissue GAG concentration

[3]. T1 relaxation enhanced by delayed administration of Gd-DTPA^{2-}, the dGEMRIC technique, can be considered the method of choice for detecting proteoglycan depletion in articular cartilage. The dGEMRIC technique has provided valuable results in clinical applications [4–6].

The reports on dGEMRIC for the postoperative evaluation of cartilage repair are scarce, limited to autologous chondrocyte implantation (ACI), and have provided controversial results [7–9]. Since GAG content is responsible for cartilage function, particularly its tensile strength, the monitoring of the development of GAG content in cartilage repair tissue in a quantitative way would be highly desirable. One reason for the controversial results is that the differences in pre-contrast values between cartilage repair tissue and normal hyaline cartilage are larger, which means the repair tissue has longer T1 values compared to normal hyaline cartilage opposed to early cartilage degeneration, where the difference has been described as small [10, 11]. Therefore, in cartilage repair tissue, the pre-contrast T1 values must be calculated, too [9, 12]. This calculation is represented by delta ΔR1, i.e., the difference in relaxation rate (R1=1/T1) between $T1_{precontrast}$ and $T1_{postcontrast.}$ [9, 12]. Thus, the sequence must be performed twice, for precontrast T1 mapping and delayed postcontrast MR T1 mapping, which increases the total data acquisition time.

In addition, the standard dGEMRIC technique is still limited to single slices in 2D acquisition and is time-consuming in 3D sequences, which detracts from its widespread clinical use.

The aim of our study was to evaluate the relative GAG content in repair tissue in patients after microfracturing (MFX) and matrix-associated autologous chondrocyte transplantation (MACT) of the knee joint with a dGEMRIC technique based on a newly developed short 3D-GRE sequence with two flip angle excitation pulses and to validate the technique against a standard inversion recovery sequence.

Materials and methods

Phantom study

The phantom study, as well as the clinical study, was performed on the same 3 T Tim Trio scanner (Siemens, Erlangen, Germany). For both phantom and clinical studies, the same dedicated eight-channel knee coil (In vivo, Gainesville, FL) was used. Phantom probes were prepared from seven different concentrations of NaCl and gadopentate dimeglumine (Magnevist, Schering, Berlin, Germany). Different Magnevist concentrations were prepared with regard to the expected range of T1 values (200 ms–1,250 ms), which are typical for pre- and postcontrast in vivo human cartilage at 3 T [13]. Initial concentrations of NaCl and Magnevist were estimated using experience from our previous studies and were optimized for our needs by an iterative process in several steps.

T1 IR

In order to calibrate the phantom fluids, an inversion recovery sequence was performed at seven different non-equidistant TI times: 25, 75, 180, 350, 650, 1100, and 1680 ms. Sixteen 2D slices with a matrix size of 256×256, a field of view (FOV) of 120×120 mm, and a 2-mm slice thickness were measured. A bandwidth of 260 Hz/pixel was used.

Nonlinear, two-parametric LS-fit using IDL (RSI, Boulder, CO) software was used for T1 map calculation. A pixel-by-pixel approach was used for the T1 map calculation. The fitting was, therefore, repeated for each of the 256×256 pixels. By using the above-mentioned software, plotted points were fitted to the expected equation for T1 IR relaxation: abs[PD*(1–2*exp(-t/T1))], where the "PD" parameter is the proton density of the measured sample, "t" is the variable that includes IR times, and T1 is the unknown relaxation parameter. Each of these fittings was repeated many times until the least-squares error reached its minimum. The final T1 map was constructed based on fitting for each individual pixel. The "MPcurvefit" IDL routine was used for fitting (Craig B. Markwardt, NASA/GSFC Code 662, Greenbelt, MD 20770). ROIs were drawn manually within each phantom and each slice. The resulting data were statistically analyzed and are summarized in the Tables 1 and 2. Phantoms were made of liquid, therefore homogeneous. Syringes were completely filled with liquid, preventing possible problems with bubbles and mixing of the liquid, as a consequence of the gradient shaking. Syringes were positioned longitudinally-along B0 direction and measured in axial orientation. ROIs were drawn in circular shapes, covering appoximately 50% of the syringe image, corresponding approximately to 500 pixels. ROIs were saved and applied (re-positioned) to every syringe image in the same way. Mean value and stardard deviation were recorded and statistically analyzed.

Dual flip angle technique

The 3D dual flip angle rf-spoiled GRE sequence for the dGEMRIC technique was used for the evaluation of the same probes. A 24.7°/4.4° flip angle combination was used. The parameters of the 3D GRE sequence were: TR/TE (ms): 15/2.86; matrix size: 256×256; FOV (mm): 120×120. The effective slice thickness was 2 mm, and 16 slices were measured. The nominal resolution was 0.46×0.46×2 mm. A bandwidth of 210 Hz/pixel was used. Measurement time was 4 min 3 s.

T1 maps were calculated using formula (1), and ROIs were drawn manually within each phantom and each slice, similar to the IR evaluation. Direct comparison of the T1 values from the 3D dual flip angle dGEMRIC technique and the IR technique was performed. The mean values and standard deviations of the numerical values of T1 relax-

ation time constants from the IR measurements and from the 3D dual flip angle GRE measurements were compared and graphically summarized.

In vivo study

Patient population

Twenty patients (2 female, 18 male; mean age of 37.3± 12.5 years; age range 19 to 66 years) treated with MFX or MACT (10 in each group) were enrolled in this study. From a larger cohort, each MFX patient was matched with one MACT patient of about the same age, the same defect localization, and the same postoperative interval for better comparability. Matching was done by means of age (MFX: 37.1±16.3 years; MACT: 37.4±8.2 years) and postoperative interval (MFX: 33.0±17.3 months; MACT: 32.0± 17.2 months).

Ethics approval for this study was provided by the Medical University ethics commission, and written informed consent was obtained from all patients prior to enrollment in the study.

For inclusion into the study, the patients of both groups had to have a single, symptomatic, full-thickness cartilage defect on the femoral condyle. Exclusion criteria were advanced or severe osteoarthritis, instability, or deformity. The solitary nature of the cartilage defect and the lack of advanced or severe osteoarthritis was preoperatively defined through conventional radiographs and MRI, and intraoperatively proven and documented at the time of surgical repair. Instability and deformity were excluded by clinical evaluation. In both groups, the cartilage defect was located on the medial femoral condyle in eight patients and on the lateral femoral condyle in two patients. Mean defect size for the MFX group was 2.82 cm2 (range: 1.8–5.1 cm2) and 5.12 cm2 (range: 2.4–9.1 cm2) for the MACT group.

Microfracture was performed as described by Steadman et al. [14]. During arthroscopy, loose cartilage bodies were removed, and marginally attached cartilage was debrided. After exact preparation of the bed, an arthroscopic 70°-angled awl was used to penetrate the subchondral plate and to generate micro-holes in the exposed bone starting in the periphery of the lesion. Subchondral plate integrity was ensured by maintaining a minimum distance of 3 mm between the micro-holes.

For MACT, Hyalograft®C, a hyaluronan-based scaffold (Fidia Advanced Biopolymers, Abano Terme, Italy) was used. Further technological advances have led to the third generation of ACI, which uses biomaterials seeded with chondrocytes as carriers and scaffolds for cell growth. These “all-in-one” grafts do not need a periosteal cover or fixing stitches and can be trimmed to exactly fit the cartilage defect. The advantages of these new techniques are their technical simplicity, shorter operating time, and the potential to perform the surgery via a mini-arthrotomy. Hyalograft®C is composed of autologous chondrocytes grown on a 3D HYAFF 11 scaffold, which promotes the in vitro proliferation of chondrocytes and favors the expression and maintenance of a cell-differentiated phenotype [15]. Surgery on all MACT patients was performed by one surgeon and surgery of all MFX patients by one other surgeon. Within their treatment group, all patients after MACT as well as all patients after MFX underwent the same rehabilitation program following accepted modern protocols [16, 17].

Image acquisition

MRI was performed on the same 3 T MR scanner (Magnetom Tim Trio, Siemens Medical Solutions, Erlangen, Germany), with a gradient strength of 40mT/m, using a dedicated eight-channel, high-resolution knee array coil (In vivo, Gainesville, FL), which was also used for the phantom study. Special attention was paid to ensure that all patients were positioned consistently in a reproducible fashion with the joint space of the extended knee in the middle of the coil.

An isotropic 3D-double echo steady state (DESS) sequence, with a TR/TE of 15.1/5.1 ms and flip angle of 25°, was used for morphological evaluation. The field of view (FoV) was 150×150 mm, the pixel matrix was 250× 250, and the isotropic voxel size was 0.6×0.6×0.6 mm. Total data acquisition time for this sequence was 6:32 min. After multiplanar reconstruction of the isotropic 3D-DESS using a 3D viewing tool, the cartilage repair site was identified to facilitate planning of appropriate anatomic coverage/localization of subsequent 3D dGEMRIC T1 mapping acquisitions.

For quantitative T1 mapping, a 3D GRE sequence with a TR: 15 ms, TE:3.15 ms, a field of view (FOV) of 160× 160 mm, and a matrix size of 448×448 was performed, resulting in a resolution in plane of 0.36×0.36 mm with an effective slice thickness of 3 mm. One slab with 16 slices was applied. The bandwidth was 210 Hz/pixel. One acquisition was used. The scan time was 4 min 3 s. Both flip angle excitation pulses (24.7° and 4.4°) were performed within the same sequence before and after intravenous administration of anionic Gd-DTPA (2-) (Magnevist, Schering, Berlin, Germany). The post-contrast MR imaging protocol reported by Burstein et al. [11] was followed, i.e., a bolus injection of 0.2 mmol per kilogram body weight Gd-DTPA (2-). After injection, the patient exercised the knee by walking up and down stairs for 20 min. Post-contrast MR imaging was performed about 90 min after administration of the contrast agent. Images were obtained in the sagittal plane for the femoro-tibial compartment. For post-contrast imaging, care was taken to perform the same slab orientation as that in the pre-contrast scan in each patient. This was accomplished by using the 3D data set of the DESS sequence to reposition in the identical plane for the dual flip angle excitation pulse GRE sequence.

Data analysis

The images were analyzed by two musculoskeletal observers blinded to the different patient groups. All images were analyzed in consensus. The graft area was identified with the morphological images provided by the DESS sequence and, in MFX patients, by visualization of alterations of the subchondral bone. In all patients, two sagittal slices covering the cartilage repair area were selected on the T1 map images and used for further analysis.

From the results of the phantom study, the slab was positioned with the graft in a central location, and the ROIs were placed completely within the region of repair tissue. In each selected slice, ROIs were manually drawn within the region of the graft area, with a mean pixel count of 455±141. To standardize the procedure, all ROIs were manually drawn by a single investigator.

For reference purposes, a remote region of morphologically normal-appearing cartilage in the same knee joint was selected and was evaluated. Since, in most cases the repair tissue was located at the weight-bearing zone, an intact cartilage area near the location of the femoral condyle of the same compartment was selected, but always with a minimum of 1 cm distance from the repair tissue. The ROI in the normal cartilage was of a size similar to the ROI in the repair tissue (446±132). The normal appearance of each reference site was verified by the isotropic 3D DESS sequence. To detect a potential variation of normal-appearing cartilage based on the age of the patients, correlation of control cartilage sites to age was also performed.

For inter-group comparison, the group mean T1 relaxation times from all ROIs within the cartilage repair tissue for each group were calculated. Values were also compared to the mean values of T1 relaxation times from all ROIs of the cartilage reference site within each group.

With the two-angle approach, the T1 map can be calculated on a pixel-by-pixel basis (using in-line software supplied by Siemens Medical Solutions, Erlangen, Germany) according to the following formula

$$T1c_{j,k} = \frac{TR}{1n\left[\frac{\sin(\alpha_1)*\cos(\alpha_2) - Q_{j,k}\sin(\alpha_2)*\cos(\alpha_1)}{\sin(\alpha_1) - Q_{j,k}*\sin(\alpha_2)}\right]}$$
$$Q_{j,k} = \frac{mess\_1_{j,k}}{mess\_2_{j,k}} \quad (1)$$

where $T1c_{j,k}$ = T1-value and $Q_{j,k}$ = the quotient of the two signal intensities for the pixel (j,k).

No filtering was applied to the images. The cartilage regions were segmented manually.

Quantitative R1=1/T1 (in 1/s) measurements were performed. In accordance with recent reports [9, 12], measurements of relaxation rate before contrast administration ($R1_{pre\text{-}contrast}$), relaxation rate after contrast administration ($R1_{post\text{-}contrast}$), and the difference between $R1_{pre\text{-}contrast}$ and $R1_{post\text{-}contrast}$ ($\Delta R1 = R1_{post\text{-}contrast} - R1_{pre\text{-}contrast}$) were obtained for both repair tissue and normal hyaline cartilage in all patients at each location defined above. From these measurements, the relative $\Delta R1=[\Delta R1_{repair\ tissue}/\Delta R1_{normal\ cartilage}]$ was calculated.

Clinical outcome

To evaluate the clinical outcome for each patient at the same time point compared to MRI, knee function was assessed using the Lysholm score [18], a scoring system that divides clinical outcome into groups of excellent, good, fair, and poor outcome. The Lysholm knee scale is a condition-specific outcome measure validated for chondral disorders of the knee, including parameters such as pain, instability, walking abnormalities, and swelling [19]. The Lysholm score was performed within the same day of the MR examination.

Statistical analysis

Considering the different measurements within each patient, an analysis of variance using a three-way ANOVA with random factors was performed. For correlation measurements, a Pearson coefficient was achieved. Statistical analyses were done using SPSS version 15.0 (SPSS Institute, Chicago, IL) for Windows (Microsoft, Redmond, WA). Differences between cartilage repair regions and normal hyaline cartilage sites, as well as Pearson correlations with a p-value less than 0.05, were considered statistically significant. Due to the small number of patients, statistical analysis within each group was obtained for all measured ROIs together.

Illustrations

Illustrations with color-coded cartilage were prepared using Adobe Photoshop graphics software. Grayscale image and color-coded images, as produced during processing by the IDL software, were loaded into Adobe Photoshop in overlaid layers. Manual cartilage segmentation was subsequently performed in grayscale images. The selection was saved and applied to the color-coded image. The segmented portion of the color-coded image was cut and pasted automatically to the same place in the grayscale

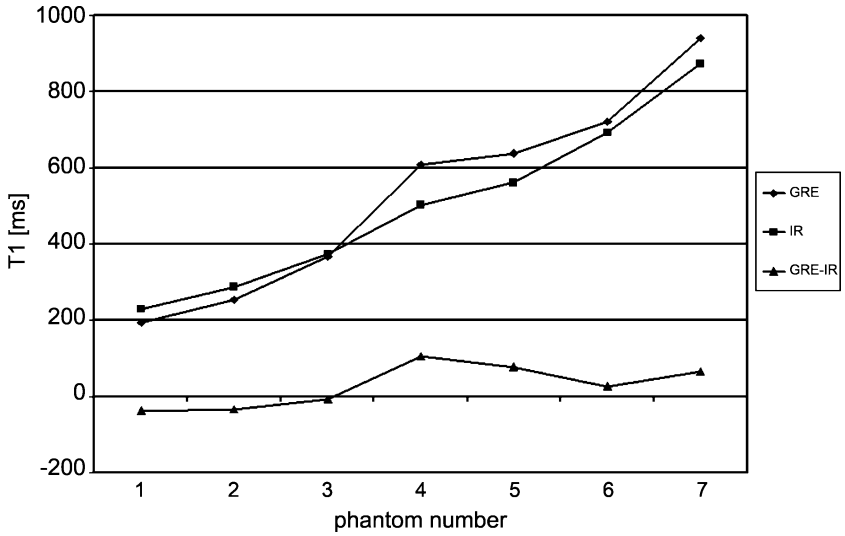

Fig. 1 Comparison of the T1 IR and the T1 variable flip angle GRE technique for seven different phantoms with a T1 from 200 ms of sample 1 and up to 875 ms of sample 7

image. In this way, correct placement of the color-coded cartilage on the grayscale image was guaranteed.

Results

Phantom study

The correlation of T1 values obtained from the IR and dual flip angle techniques, with an excitation pulse combination of 24.7°/4.4° degrees, is shown on Fig. 1. Corresponding T1 values are listed in Table 1. There was an apparent slice profile effect, where the center of the excited slab had a correct flip angle, but the edges of the RF coil did not. Consequently of 16 slices measured over the phantom, the central 10 slices showed a correlation with IR, and 6 outer slices correlated poorly due to B1 heterogeneity at the periphery of the coil (Fig. 2).

Patient study

An example of color-coded T1 relaxation time maps before and after intravenous contrast agent administration in a patient 31 months after MACT surgery shows different T1 values at the cartilage repair site compared to adjacent normal hyaline cartilage ($p=0.001$; ANOVA F-value 13.3) (Fig. 3a,b). The difference between pre- and postoperative T1 values in a patient 32 months after microfracture surgery for cartilage repair is even more apparent ($p<0.001$; ANOVA F-value 63.9) (Fig. 4a,b).

The pre- and post-contrast relaxation rates for two representative patients, one after MFX and a second one after MACT, are listed in Table 2.

The mean $\Delta R1$ for MFX was 1.07 ± 0.34 versus 0.32 ± 0.20 at the intact control site, and 1.90 ± 0.49 for MACT compared to 0.87 ± 0.44, which resulted in a relative $\Delta R1$ of 3.39 for MFX and 2.18 for MACT. The difference between the cartilage repair groups was statistically significant ($p=0.013$; ANOVA F-value 7.1). In addition, with regard to the age of the patients and healthy-appearing cartilage sites, no correlation could be found.

Clinical outcome

Based on Lysholm scoring, clinical outcome assessments of the MACT and MFX patients showed no significant differences between the two cartilage repair procedures ($p>0.05$). In patients after MACT and in patients after MFX, nine patients of each group showed excellent and

Table 1 Phantom study performed using the T1 GRE technique and the gold-standard T1 IR technique

Sample no.:	1	2	3	4	5	6	7
T1 GRE [ms]	193.7	254.4	366.4	607.6	637.8	720.1	939.7
T1 IR [ms]	230.1	287.8	372.3	502.2	560.8	692.4	872.6
Relative error [%]	−16	−12	−2	21	14	4	8

Seven samples with different contrast agent concentrations were measured and evaluated. Relative error in % shows good correlation of these two techniques

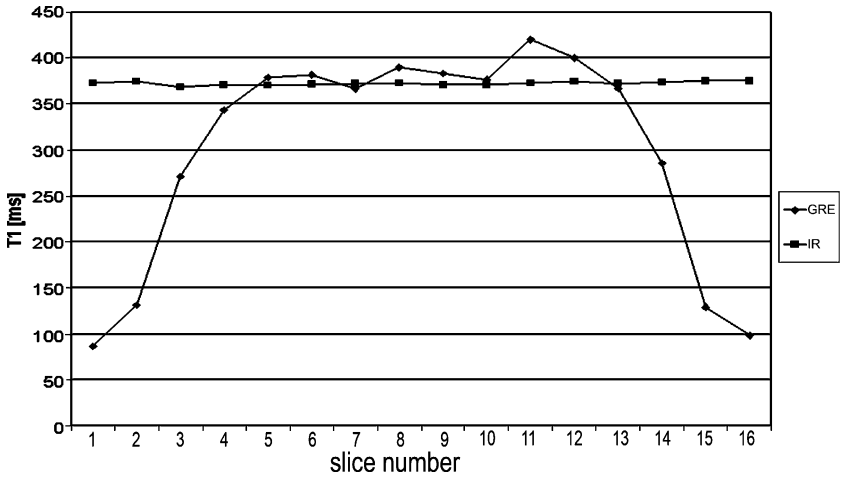

Fig. 2 Comparative measurement of variable flip angle GRE technique in a phantom sample 3 of 372 ms. The variable flip angle GRE technique is more sensitive to the excitation profile. Therefore, only 10 central slices of a total of 16 slices are useful for T1 evaluation and show acceptable correlation with the IR technique

good results, respectively, and one patient in both groups showed poor results.

Discussion

Similar to a recent report [20], we used a rf-spoiled 3D-gradient echo sequence with two different flip angle excitation pulses for T1 mapping. In comparison to this report, a very short data acquisition time of 4 min 3 s could be achieved, and the sequence did not have to be performed twice, since both flip angle excitation pulses are integrated within one sequence. As another benefit, the phantom study performed with this sequence demonstrated a lower sensitivity to the excitation profile resulting in 10 of 16 slices with reliable T1 values compared to the reference inversion recovery technique, whereas in the previous study this was true for 8 of 16 slices [20]. These differences to the reported dual-flip angle technique, in particular the significant reduction in data acquisition time, makes this sequence highly attractive for clinical applications.

T1 mapping for the dGEMRIC technique is usually based on progressive inversion or saturation of the longitudinal magnetization, with at least two data sets with different T1-relevant parameters to determine the T1 parameter maps. Both these sequence types are mainly based on 2D acquisition schemes and therefore necessitate relatively thick slices. Another drawback is the relatively long acquisition times required. Another technique for fast T1 mapping is to use the contrast variation of different excitation flip angle values in gradient echo-based sequences [21, 22]. The gradient echo method with

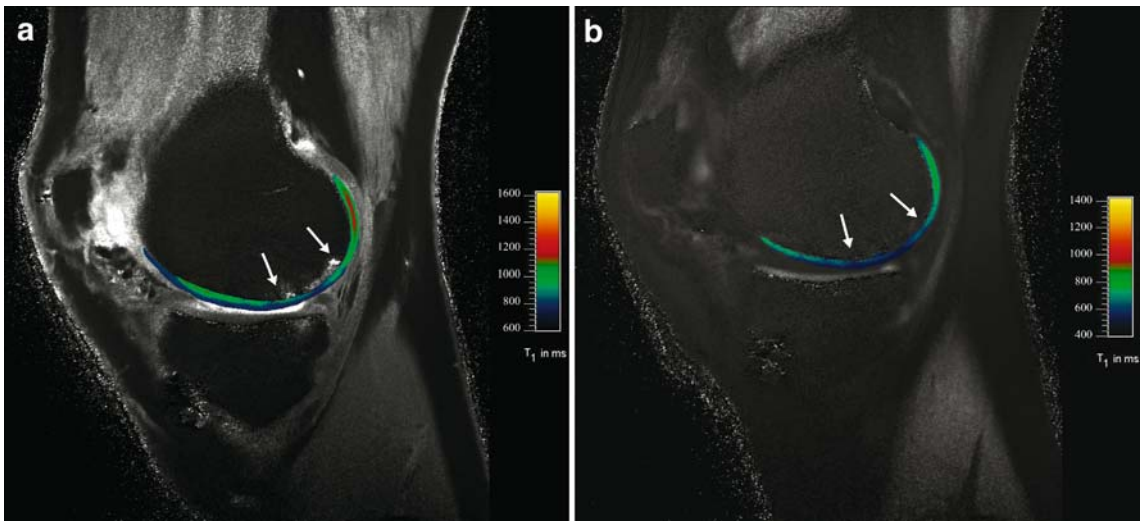

Fig. 3 **a** Color-coded cartilage transplant pre-contrast is shown in A. The 3D, dual flip angle dGEMRIC technique was applied in a 34-year-old male patient 32 months after MACT. There are slightly lower T1 values in the cartilage transplant region, compared to normal cartilage. White arrows mark the borders of the transplant. **b** Shows color-coded cartilage repair tissue post-contrast. The figure shows lower T1 values of the T1 map for cartilage transplant after intravenous administration of contrast agent. White arrows mark the borders of the transplant

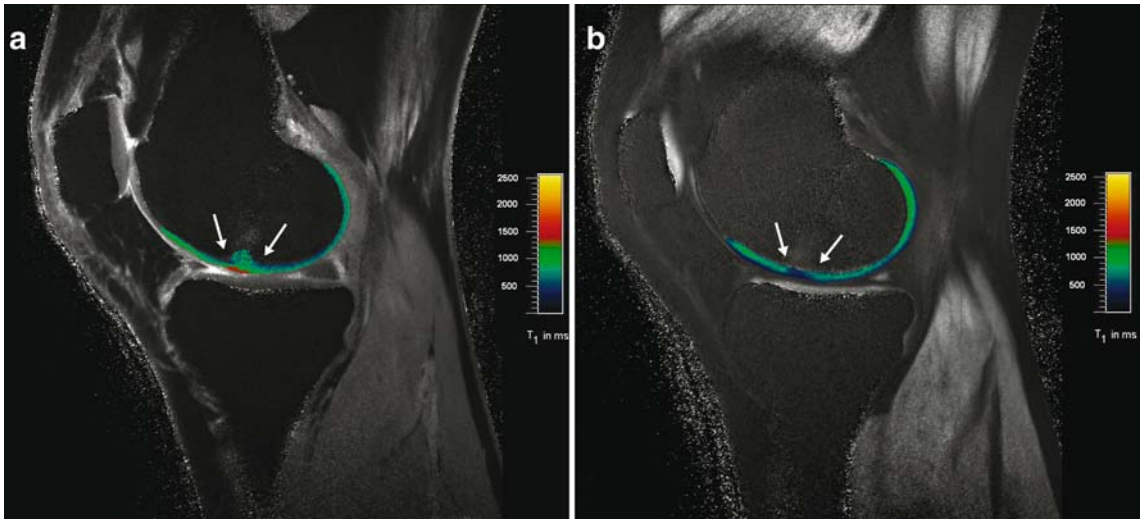

Fig. 4 **a** Color-coded cartilage repair tissue pre-contrast is shown in A. The 3D, dual flip angle dGEMRIC technique was applied in a 36-year-old male patient 31 months after MFX. There are similar T1 values in cartilage repair tissue, compared to normal cartilage. White arrows mark the borders of the repair tissue. **b** Color-coded cartilage repair tissue following intravenous contrast agent. The figure shows the corresponding T1 map after enhancement, with marked lower T1 values in the repair tissue. White arrows mark the borders of the transplant

variable flip angles has been reported previously; however, in earlier studies, poor reproducibility due to partial volume effects and unstable signal intensity of the first and second images due to sub-optimal flip angles were reported [23–26]. The subsequent effect is further enhanced by noise-induced bias, which can be found below a certain signal-to-noise ratio (SNR). In the technique reported in this study, care was taken to position the graft in the center of the slab, allowing central slices to be used, which eliminates partial volume effects and increases the SNR.

New generations of autologous chondrocyte implantation (ACI) have been developed for surgical therapy of larger cartilage defects to decrease the number of complications associated with classical ACI, such as graft hypertrophy and delamination. These new generations of ACI, called matrix-associated autologous chondrocyte transplantation (MACT), are based on the use of biodegradable scaffolds or polymers and seem to be promising with respect to a lower rate of complications. Furthermore, the matrices used seem to favor differentiation of chondrocytes [15, 27]. Another frequently used treatment for the repair of articular cartilage lesions of the knee is the microfracture (MFX) technique [28, 29]. With this method, the subchondral bone is penetrated to allow fibrin clot formation within the defect and the subsequent maturation of repair tissue, which fills the cartilage defect. The role of bone marrow stimulating techniques, such as microfracture, as an alternative to autologous chondrocyte implantation, is not yet thoroughly defined [30].

In addition to morphological MR imaging of cartilage repair tissue, an advanced method to non-destructively and quantitatively monitor the parameters that reflect the biochemical status of cartilage repair tissue is the necessity for studies that seek to elucidate the natural maturation of surgical cartilage grafts and the efficacy of these techniques. Two promising techniques are T2 mapping, which reflects water content, collagen organization, and content,

Table 2 Exemplary T1 values of patients after MFX and MACT

	Control [ms]		TX [ms]		Control [1/s]			TX [1/s]			
	Pre	Post	Pre	Post	R1 pre	R1 post	Δ R1	R1 pre	R1 post	Δ R1	Rel. Δ R1
Patient 1	1,219	772	1,202	457	0.82	1.30	0.47	0.83	2.19	1.36	2.85
	1,146	643	1,217	428	0.87	1.56	0.68	0.82	2.34	1.51	2.22
Patient 2	1,190	572	1,080	450	0.84	1.75	0.91	0.93	2.22	1.30	1.42
	1,257	645	1,156	480	0.80	1.55	0.75	0.87	2.08	1.22	1.61

Both male patients, both 46 years old; 48 months after MFX (patient 1) and 52 months after MACT (patient 2)
In both patients the cartilage repair area is located in the weight-bearing zone of the medial femoral condyle. The T1 values, R1 values, ΔR1 values and relative ΔR1 in cartilage repair tissue compared to the reference hyaline cartilage tissue are listed

and dGEMRIC for T1 mapping, which is specific for GAG content [31–35].

In the in vivo part of this study, we have shown that it is feasible to apply this 3D variable flip angle dGEMRIC technique in patients after various cartilage repair surgeries, such as MFX and MACT.

The use of dGEMRIC to monitor the GAG content in the follow-up of patients after ACI has been reported [7, 8]. Contrary to these studies, we found higher relative ΔR1 values that reflect an even lower GAG content in the repair tissue in MACT, with a mean of 33 months after surgery. One possible explanation may be that, in these studies, MR imaging and mapping were only performed after the adminstration of contrast agent, and, therefore, an overestimation of the GAG content in the repair tissue may have occurred. In the study by Watanabe et al. only the calculation of the relative ΔR1 values showed a correlation with the GAG content in cartilage implants using gas chromatography of biopsy samples as standard of reference [9].

From histological studies derived from biopsies, it is known that patients with MACT develop hyaline-like (although not native hyaline) repair tissue over time, while in patients with microfracture, fibrous tissue is found [36, 37].

The repair tissue formed with a microfracture procedure contains less PG and an abnormal distribution of collagen compared to normal cartilage, which may explain the resultant poor mechanical properties often exhibited by repair tissue in the long term [38, 39].

Still, a comparison of periost-related ACI and MFX in 80 patients did not demonstrate a significant difference between the respective techniques in the Lysholm score [30]. Conversly, biopsy assessment of 67 patients showed that ACI results in hyaline-like repair tissue more frequently than MFX. Results of our study correspond well with these data. Whereas there is no significant difference in the Lysholm score between ACI and MFX patients, MR findings on T1 mapping demonstrate significantly higher relative ΔR1 in microfracture compared to MACT, which corresponds to a lower GAG content.

One limitation of the current study is that histological specimens were not available for direct comparison. Due to the described good clinical outcome, no arthroscopy was performed in these patients, and the integrity of the reference site was defined based on standard cartilage MR imaging. In addition, the correlation between control cartilage sites and age showed no significant results, indicating no dependence of healthy cartilage to possible degeneration because of age. This statement, however, must be evaluated further in much larger cohorts of healthy volunteers. The difference in the ΔR1 values of normal cartilage in the two patient groups seems to reflect the variability of these values in healthy cartilage, which was recently reported [4]. Williams et al. found mean ΔR1 values of 0.61±0.19, with a range from 0.08–0.90 [4]. These values lie in between the values of the two control values of our two post surgical groups. This underlines the importance of the calculation of individual ratios between repair tissue and normal cartilage, such as the relative ΔR1. An additional limitation is the low number of patients in the two groups.

In conclusion, the 3D dual flip angle dGEMRIC technique is comparable to the standard T1 inversion recovery technique for T1 mapping, and an assessment of GAG content in repair tissue produced by two different cartilage surgery techniques is feasible and can be performed in a short data acquisition time.

Acknowledgements Contract grant sponsor: Austrian Science Fund (FWF); contract grant number: FWF-Projekt P18110-B15.

References

1. Lohmander LS (1994) Articular cartilage and osteoarthrosis. The role of molecular markers to monitor breakdown, repair and disease. J Anat 184(Pt 3):477–492
2. Burstein D, Bashir A, Gray ML (2000) MRI techniques in early stages of cartilage disease. Invest Radiol 35 (10):622–638 Review
3. Bashir A, Gray ML, Boutin RD, Burstein D (1997) Glycosaminoglycan in articular cartilage: In vivo assessment with delayed Gd(DTPA)(2-)-enhanced MR imaging. Radiology 205 (2):551–558
4. Williams A, Gillis A, McKenzie C et al (2004) Glycosaminoglycan distribution in cartilage as determined by delayed gadolinium-enhanced MRI of cartilage (dGEMRIC): Potential clinical applications. Am J Roentgenol 182 (1):167–172
5. Kim YJ, Jaramillo D, Millis MB, Gray ML, Burstein D (2003) Assessment of early osteoarthritis in hip dysplasia with delayed gadolinium-enhanced magnetic resonance imaging of cartilage. J Bone Joint Surg Am 85A (10):1987–1992
6. Tiderius CJ, Olsson LE, Leander P, Ekberg O, Dahlberg L (2003) Delayed gadolinium-enhanced MRI of cartilage (dGEMRIC) in early knee osteoarthritis. Magnet Reson Med 49(3):488–492
7. Gillis A, Bashir A, McKeon B, Scheller A, Gray ML, Burstein D (2001) Magnetic resonance imaging of relative glycosaminoglycan distribution in patients with autologous chondrocyte transplants. Invest Radiol 36(12):743–748
8. Kurkijarvi JE, Matilla L, Ojala RO et al (2007) Evaluation of cartilage repair in the distal femur after autologous chondrocyte transplation using T2 relaxation time and dGEMRIC. Osteoarthr Cartilage 15(4):372–378

9. Watanabe A, Wada Y, Obata T et al (2006) Delayed gadolinium-enhanced MR to determine glycosaminoglycan concentration in reparative cartilage after autologous chondrocyte implantation: Preliminary results. Radiology 239(1):201–208
10. Bashir A, Gray ML, Hartke J, Burstein D (1999) Nondestructive imaging of human cartilage glycosaminoglycan concentration by MRI. Magnet Reson Med 41(5):857–865
11. Burstein D, Velyvis J, Scott KT et al (2001) Protocol issues for delayed Gd (DTPA)(2-)-enhanced MRI: (dGEMRIC) for clinical evaluation of articular cartilage. Magnet Reson Med 45 (1):36–41
12. Tiderius CJ, Olsson LE, de Verdier H, Leander P, Ekberg O, Dahlberg L (2001) Gd-DTPA (2-)-enhanced MRI of femoral knee cartilage: A dose-response study in healthy volunteers. Magnet Reson Med 46(6):1067–1071
13. Williams A, Mikulis B, Krishnan N, Gray M, McKenzie C, Burstein D (2007) Suitability of T1Gd as the "dGEMRIC Index" at 1.5 and 3.0T. Magn Reson Med 58(4):830–834
14. Steadman JR, Rodkey WG, Singleton SB, Briggs KK (1997) Microfracture technique for full-thickness chondral defects. Technique and clinical results. Oper Tech Orthop 7:300–304
15. Marlovits S, Zeller P, Singer P, Resinger C, Vecsei V (2006) Cartilage repair: Generations of autologous chondrocyte transplantation. Eur J Radiol 57(1):24–31
16. Steadman JR, Rodkey WG, Briggs KK (2002) Microfracture to treat full-thickness chondral defects: surgical technique, rehabilitation, and outcomes. J Knee Surg 15:170–176
17. Hambly K, Bobic V, Wondrasch B, Van Assche D, Marlovits S (2006) Autologous chondrocyte implantation postoperative care and rehabilitation: science and practice. Am J Sports Med 34:1020–1038
18. Lysholm J, Gillquist J (1982) Evaluation of knee ligament surgery results with special emphasis on use of a scoring scale. Am J Sports Med 10:150–154
19. Kocher MS, Steadman JR, Briggs K, Sterett WI, Hawkins RJ (2004) Reliability, validity, and responsiveness of the Lysholm knee scale for various chondral disorders of the knee. J Bone Joint Surg Am 86-A:1139–1145
20. Trattnig S, Gebetsroither S, Szomolanyi P, Welsch GH, Salomonowitz E, Watanabe A, Deimling M, Mamisch TC (2007) Three-dimensional delayed Gadolinium enhanced MRI of cartilage (dGEMRIC) for in vivo evaluation of reparative cartilage after matrix-associated autologous chondrozyte transplantation at 3.0 Tesla - preliminary results. J Magn Reson Imaging 26:974–982
21. Kimelman T, Vu A, Storey P, McKenzie C, Burstein D, Prasad P (2006) Three dimensional T1 mapping for dGEMRIC at 3.0 T using the Look Locker method. Invest Radiol 41 (2):198–203
22. Roberts S, Isaksen V, Johansen O. Autologous ChondroBrix G, Schad LR, Deimling M, Lorenz WJ (1990) Fast and precise T1 imaging using a tomrop sequence. Magn Reson Imaging 8 (4):351–356
23. Deoni SC, Rutt BK, Peters TM (2003) Rapid combined T1 and T2 mapping using gradient recalled acquisition in the steady state. Magn Reson Med 49:515–526
24. Imran J, Langevin F, Saint-Jalmes H (1999) Two-point method for T1 estimation with optimized gradient-echo sequence. Magn Reson Imaging 17:1347–1356
25. Schmitt P, Griswold MA, Jakob PM et al (2004) Inversion recovery TrueFISP: quantification of T(1), T(2), and spin density. Magn Reson Med 51:661–667
26. Steinhoff S, Zaitsev M, Zilles K, Shah NJ (2001) Fast T(1) mapping with volume coverage. Magn Reson Med 46:131–140
27. Marcacci M, Berruto M, Brocchetta D et al (2005) Articular cartilage engineering with Hyalograft (R) C-3-year clinical results. Clin Orthop Relat Res 435:96–105
28. Steadman JR, Briggs KK, Rodrigo JJ, Kocher MS, Gill TJ, Rodkey WG (2003) Outcomes of microfracture for traumatic chondral defects of the knee: average 11-year follow-up. Arthroscopy 19:477–484
29. Gobbi A, Nunag P, Malinowski K (2005) Treatment of full thickness chondral lesions of the knee with microfracture in a group of athletes. Knee Surg Sports Traumatol Arthrosc 13:213–221
30. Knutsen G, Engebretsen L, Ludvigsen TC, Drogset JO, Grøntvedt T, Solheim E, Strand T (2004) Autologous chondrocyte Implantation compared with Microfracture in the Knee. J Bone Joint Surg Am 86-A(3):455–464
31. Burstein D, Gray ML (2006) Is MRI fullfilling ist promise for molecular imaging of cartilage in arthrits? Osteoarthritis Cartilage 14:1087–1090
32. Tiderius CJ, Svensson J, Leander P, Ola T, Dahlberg L (2004) dGEMRIC (delayed gadolinium-enhanced MRI of cartilage) indicates adaptive capacity of human knee cartilage. Magn Reson Med 51:286–2890
33. Trattnig S, Mamisch TC, Welsch GH, Glaser C, Szomolanyi P, Gebetsroither S, Stastny O, Horger W, Millington S, Marlovits S (2007) Quantitative T2 mapping of matrix-associated autologous chondrocyte transplantation at 3 Tesla: an in vivo cross-sectional study. Invest Radiol 42(6):442–448
34. Mendlik T, Faber SC, Weber J, Hohe J, Rauch E, Reiser M, Glaser C (2004) T2 quantitation of human articular cartilage in a clinical setting at 1.5 T: implementation and testing of four multiecho pulse sequence designs for validity. Invest Radiol 39(5):288–299
35. Mosher TJ, Smith HE, Collins C, Liu Y, Hancy J, Dardzinski BJ et al (2005) Change in knee cartilage T2 at MR imaging after running: a feasibility study. Radiology 234:245–249
36. Tins BJ, McCall IW, Takahashi T, Cassar-Pullicino V, Roberts S, Ashton B, Richardson J (2005) Autologous chondrocyte implantation in the knee joint: MR imaging and histologic features at 1-year follow-up. Radiology 234(2):501–508. Epub 2004 Dec 22
37. Nehrer S, Minas T (2000) Treatment of articular cartilage defects. Invest Radiol 35(10):639–646
38. Minas T, Nehrer S (1997) Current concepts in the treatment of articular cartilage defects. Orthopedics 20:525–538
39. Ghivizzani SC, Oligino TJ, Robbins PD, Evans CH (2000) Cartilage injury and repair, Phys. Med. Rehabil. Clin. North Am 11(2):289–307